JOURNAL OF MATERIALS SCIENCE 31 (1996) 5811–5815

# A model for the ⟨100⟩ crystallographic tunnel etching of aluminium

JAE-HAN JEONG
*Samsong-Research Institute, Sam-Young Electronics Co., Seong-Nam, 462-120, Korea*
CHANG-HEE CHOI, DONG NYUNG LEE
*School of Materials Science and Engineering and Centre for Advanced Materials Research, Seoul National University, Shinrim-2-dong, Kwanak-gu, Seoul 151-742, Korea*

When high purity aluminium foil is subjected to DC electrochemical etching in hot aqueous chloride solution at temperatures above 60 °C, the ⟨100⟩ crystallographic tunnel growth of an etch pit is achieved. This crystallographic tunnel growth behaviour arises due to the following reason. The tunnel tip region where the active corrosion reaction takes place tends to be made of {111} planes which minimize the surface energy, whilst the subsequent tunnel wall is made of {100} planes, because the passive oxide film formed on the {100} planes, along which the biaxial elastic modulus is the smallest, would be least attacked by corrosion.

## 1. Introduction

Anodic dissolution of high purity aluminium in hot aqueous chloride solution produces a high density of μm-wide fine tunnels which penetrate the aluminium in the ⟨100⟩ directions at rates of $\mu m\,s^{-1}$. The cross sectional size of the tunnel is constant or decreases very slowly with increasing depth. The tunnel etched aluminium foil can serve for electrodes in electrolytic capacitors [1, 2]. A number of studies have been made on the effects that the electrochemical etching variables such as the current density, electrolytic temperature and electrolyte composition have on the etch pit morphology [3–7]. According to the results of Herbert *et al.* [5], the etch tunnels grow along the ⟨100⟩ directions and the tunnel side walls are made of {100} planes. They also claimed that the metal surface at the tip of the tunnel appeared to be flat and smooth, indicating that the tip was composed of {100} planes. Having observed a similar phenomenon, Jackson [8] suggested that the directional nature of dissolution appeared to be related to the lower energy required to remove atoms from the {100} planes but gave no detailed reasons to support this idea.

Two ways to sustain the tunnel growth were proposed by Alwitt *et al.* [3]. The first is to have two parallel reactions that of tip dissolution and also wall passivation, i.e., dissolution takes place at the tip of the tunnel, whilst the side walls are passivated. The second is sequential dissolution and passivation. In the second case, a sequence consists of the initiation of a pit at the tunnel tip, pit growth and passivation of this new surface. A new breakdown takes place on the new surface and the next cycle starts. An important mechanism of the tunnel growth behaviours is passivation, that is to say, that a passive oxide film is formed on the aluminium during the electrochemical etching, whether the passivation takes place in the tunnel side walls while the tunnel tips actively corrode or the sequential passivation takes place in the tunnel side walls and tunnel tips.

The microstructure of the passive film formed on the aluminium during the electrochemical etching under high concentrations of chloride solutions at temperature above 60 °C is not clearly understood yet. However the results of Dyer *et al.* [6] showed that the passive film (in this paper, the passive film is called "etch-film") might be a hydroxide, probably in combination with an amorphous oxide. Therefore the passive film formed on aluminium during the etching is presumed to be similar to that of the hydrous oxide film produced by the reaction of aluminium in hot water. But the thickness of the passive film during the etching is much thinner than that of the hydrous oxide film formed by the reaction of aluminium in hot water. The hydrous oxide is known to be pseudo-boehmite, a poorly crystallized oxyhydroxide which is similar to boehmite (AlOOH or $Al_2O_3.H_2O$) but contains excess water [9, 10, 11, 13]. A recent study by Takahashi *et al.* [12] indicates that the inner layer of pseudoboehmite adjacent to the aluminium substrate has a very thin compact amorphous structure and the outer layer has a crystalline structure. The average composition and density of pseudoboehmite are $Al_2O_3 \cdot 2.7H_2O$ and 2.2–2.4 $g\,cm^{-3}$, respectively.

It is not known why the etch tunnels grow along the ⟨100⟩ directions and why the tunnel side walls are made of the {100} planes. In this paper the structure of the tunnels has been reexamined and a model for the ⟨100⟩ tunnel etching has been proposed.

0022–2461 © *1996 Chapman & Hall*

## 2. Experimental methods

A 100 μm thick 99.99% aluminium foil with the (100) [001] texture was subjected to DC electroetching in 1.88 M HCl solution at 80 ±2 °C. The surface of the etched aluminium was observed by scanning electron microscopy (SEM) after it was vapour coated with gold-palladium. In order to observe the growth of the etch pits, the etched aluminium foil was anodized in the 10% boric acid, 89.5% ethylene glycol and 0.5% ammonium penta-borate solution at a constant current of 2A $dm^{-2}$ up to 495 V. In this way about 650 nm of the barrier type oxide film was obtained, and the film is thought to retain the shape of the etch pits or the tunnels. The anodized specimen was broken and any unoxidized aluminium was dissolved out in a 40% $HNO_3$ solution over 8 hrs. The broken specimen was observed under SEM after it was vapour coated with gold-palladium.

A conventional method of observing the morphology of an etch-pit or tunnels is an anodizing technique. In the technique the etched aluminium foil is anodized up to 50–100 V at a constant current, and then the unoxidized aluminium is selectively dissolved in hot aqueous bromine/methanol solution. In this way an oxide replica film is obtained. The drawback of this anodizing technique is that the initial morphology of the etch pits or the tunnels may not be retained because the density of aluminium is different from that of aluminium oxide and also sharp corners tend to become blunted.

Therefore a new method of observing the morphology of the pits or tunnels has been attempted. The method consists of replicating the tunnels by the electrodeposition of copper into the tunnels. The electrodeposition condition is given in Table I.

Aluminium in the electrodeposited foil was dissolved out in a 1N NaOH solution and the copper replica of the etch tunnels was observed under SEM without the gold-palladium coating.

## 3. Results

Fig. 1 shows square pits formed on the etched aluminium foil. Fig. 2 shows a microstructure of the etched foil sectioned along a direction normal to the foil plane. The columns in Fig. 2 are oxides, anodically formed around the etch tunnels. They indicate the ⟨100⟩ directional growth of tunnels. A magnified picture of the tunnel tip clearly shows its shape and size (Fig. 3). However, the anodizing technique cannot give us accurate information on the size and shape of tunnels because the anodic oxide layer can grow into both sides of the tunnel walls.

TABLE I Electrodeposition condition for copper replication

| |
|---|
| cathode: etched aluminium foil |
| anode: platinum |
| bath compositions: 0.75 M $CuSO_4 \cdot 5H_2O$, 75 $g\,l^{-1}$ $H_2SO_4$, 0.2 $g^{-1}$ gelatine |
| apparent cathode current density: 2A $dm^{-2}$ |
| electrolysis time: 8 h |

The copper replica technique described in the previous section reveals a more accurate morphology of the tunnels as is shown in Fig. 4. The figure shows that some tunnels have a square cross section, indicating that the tunnel walls are composed of {100} planes in agreement with earlier workers' results [5]. However, the tunnels do not have flat fronts as presumed by Herbert *et al.* [5] and Jackson [8] as shown in Fig. 5. The front tunnel tip is rather sharp and appears to consist of {111} planes. Fig. 5 shows that the cross section of the tunnel is circular rather than square. Higher temperatures tend to make circular tunnels. Occasionally it can be seen that the diameter of the front region of the tunnels is slightly larger than that of the back part (Fig. 5).

## 4. Discussion

As mentioned previously, Alwitt *et al.* [3] proposed two ways to sustain the tunnel growth. One is parallel reactions of tip dissolution and wall passivation, and the other one is sequential dissolution and passivation. Our experimental results appear to support the first mechanism. Fig. 5 shows that the tunnel tip surface consists of {111} planes and the maximum dimension of the tip zone is followed by slightly smaller dimension of the tunnel. The smaller dimension

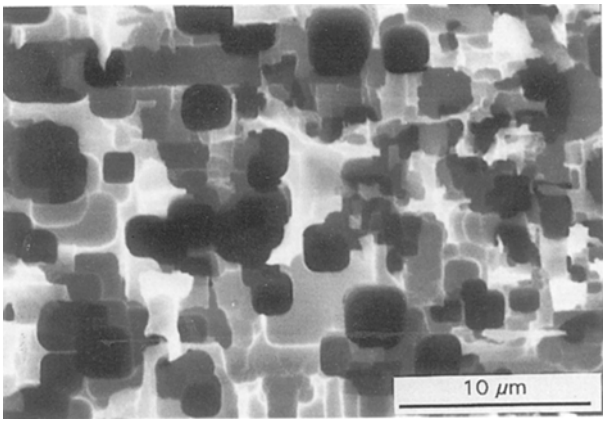


*Figure 1* Microstructure of an aluminium surface showing square etch pits.

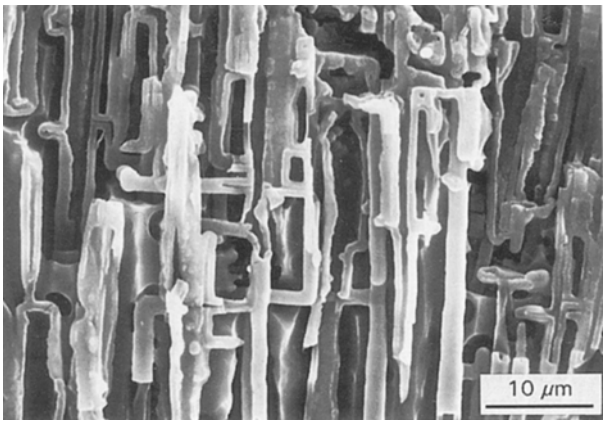


*Figure 2* Microstructure of the cross section of etched and anodized aluminium foil.

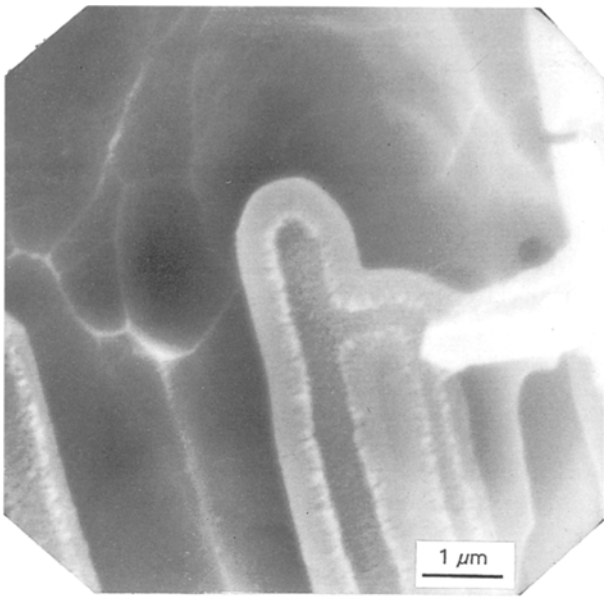


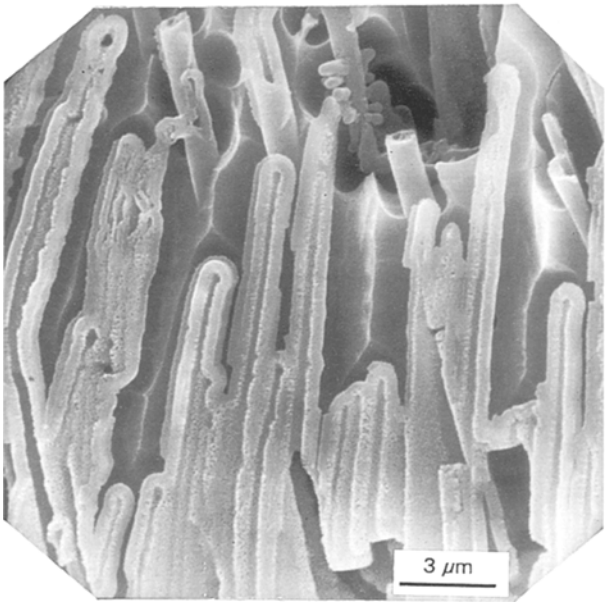


*Figure 3* Magnified pictures of tunnel tips.

implies that the passive oxide film has been formed on the wall, while dissolution takes place at the tip. From Fig. 5 the passive oxide film is estimated to be about 0.1 μm thick.

If the passive film forms on the wall, a natural misfit exists between the film and the aluminium substrate, which in turn gives rise to stress in both the film and the substrate. The film on an elastically soft substrate will be less stressed and more stable than that on an elastically hard substrate.

The stress state of the film is approximated to be biaxial, because the thickness of the film is very thin but the substrate is under the more complex stress state. However, for the purpose of comparison, the stress state of the substrate layer near the film-substrate interface was assumed to be under a biaxial stress state, and the biaxial moduli of various lattice planes of aluminium were calculated and are shown in Fig. 6. (The calculation procedure of the biaxial elastic modulus is given in the appendix). From the values in

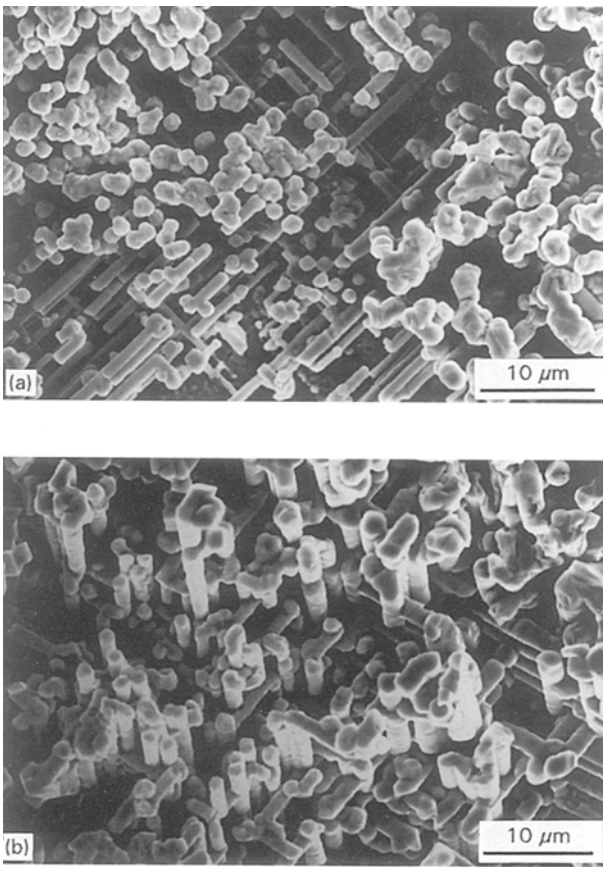


*Figure 4* Microstructures of each tunnels replicated by electrodeposition of copper. (a) Top view (b) Skewed view.

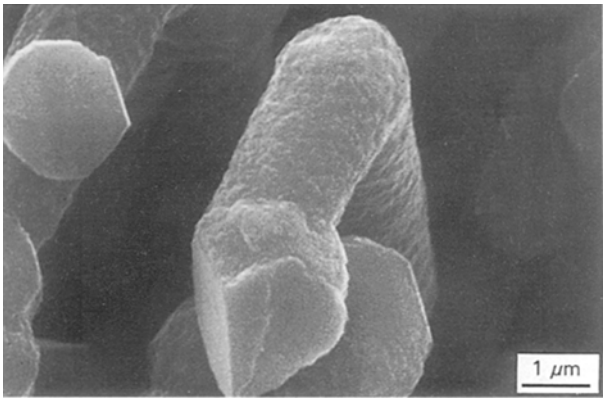


*Figure 5* Micrograph showing that the tunnel tips are composed of {111} planes.

Fig. 6, it can be seen that the minimum biaxial elastic modulus is obtained in the (100) plane. Therefore the passive film on the (100) plane would be the most stable and least attacked. It follows that the tunnel wall would consist of {100} planes. Meanwhile, the tunnel tip, where active corrosion takes place, would tend to be made of four closely packed {111} planes in order to minimize the surface energy. These situations are depicted in Fig. 7, which implies ⟨100⟩ tunnel etching.

## 5. Conclusions

The ⟨100⟩ tunnel etching of aluminium when subjected to DC electroetching in HCl solution at 80 °C is

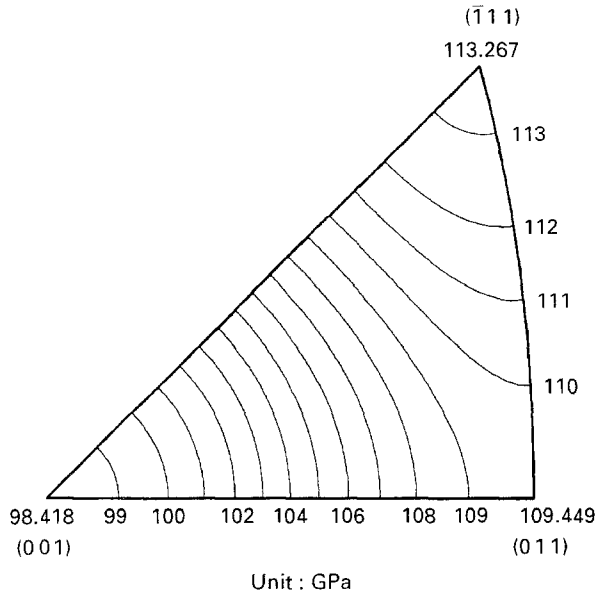


*Figure 6* Calculated average biaxial elastic modulus contours of aluminium.

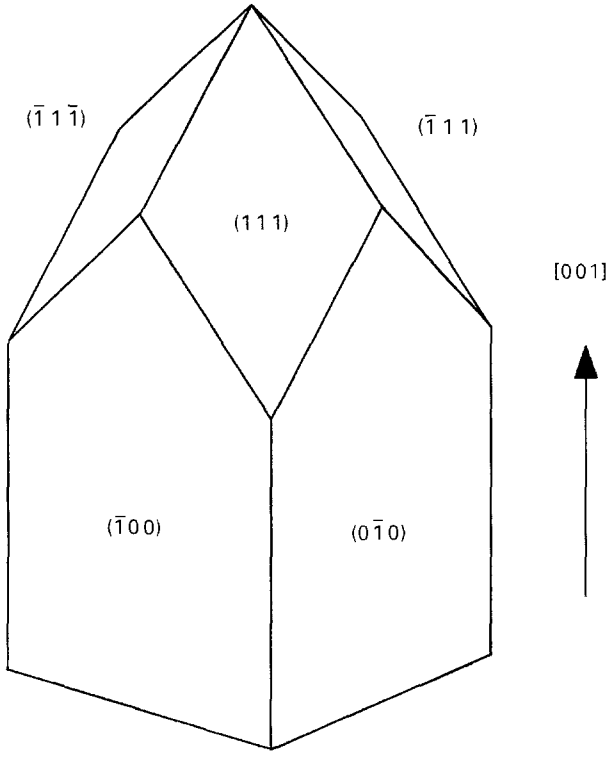


*Figure 7* A schematic illustration of a proposed tunnel growth. Arrow indicates the growth direction.

attributed to the fact that the tunnel tip region, where the active corrosion reaction takes place, tends to be made of {111} planes in order to minimize the surface energy, whilst the subsequent tunnel wall is made up of {100} planes, because the passive oxide film is formed on the plane, along which the biaxial elastic modulus is smallest and therefore would be least attacked by corrosion.

## Acknowledgement

This work has been supported by the Korea Science and Engineering Foundation through Research Centre for Thin Film Fabrication and Crystal Growing of Advanced Materials, Seoul National University.

## Appendix

For a material under a uniaxial stress, the Young's modulus $E$ is interpreted as a stiffness of the material. An elastically hard material under a uniaxial stress has a larger Young's modulus and a larger strain energy than an elastically soft material. The relations between stress $\sigma$ and strain $\varepsilon$, and strain energy $W$ are given by

$$\sigma = E\varepsilon \tag{1}$$

$$W = \tfrac{1}{2}E\varepsilon^2 \tag{2}$$

For a thin material under an equibiaxial plane stress, the stress state can be expressed as

$$\sigma'_{11} = \sigma'_{22} = \sigma \tag{3}$$

where $\sigma'_{11}$ and $\sigma'_{22}$ are the stresses along arbitrary axes $x'_1$ and $x'_2$.

The strain required to produce the stresses are given by

$$\varepsilon'_{11} = S'_{11}\sigma'_{11} + S'_{12}\sigma'_{22} \tag{4}$$

$$\varepsilon'_{22} = S'_{12}\sigma'_{11} + S'_{22}\sigma'_{22} \tag{5}$$

where the compliances, $S'_{11}, S'_{12}$ and $S'_{22}$, can be expressed in terms of the compliances $S_{ij}$ referred to the basic symmetry axes of the materials using the transformations law as follows:

$$S'_{11} = S_{11} - 2(S_{11} - S_{12} - S_{44}/2)(a_{11}^2a_{12}^2 + a_{12}^2a_{13}^2 + a_{13}^2a_{11}^2) \tag{6}$$

$$S'_{12} = S_{12} + (S_{11} - S_{12} - S_{44}/2)(a_{11}^2a_{21}^2 + a_{12}^2a_{22}^2 + a_{13}^2a_{23}^2) \tag{7}$$

$$S'_{22} = S_{11} - 2(S_{11} - S_{12} - S_{44}/2)(a_{21}^2a_{22}^2 + a_{22}^2a_{23}^2 + a_{23}^2a_{21}^2) \tag{8}$$

where the direction cosines $a_{ij}$ relate an arbitrary direction $x'_i$ to the symmetry axes $x_j$.

In the equibiaxial strain condition that

$$\varepsilon'_{11} = \varepsilon'_{22} = \varepsilon = S'_{11}\sigma'_{11} + S'_{12}\sigma'_{22} = S'_{12}\sigma'_{11} + S'_{22}\sigma'_{22}$$

or

$$(S'_{11} - S'_{12})\sigma'_{11} = (S'_{22} - S'_{12})\sigma'_{22} \tag{9}$$

Therefore

$$\varepsilon = \left(S'_{11} + S'_{12}\frac{S'_{11} - S'_{12}}{S'_{22} - S'_{12}}\right)\sigma'_{11} = \frac{1}{M_1}\sigma'_{11} \tag{10}$$

$$\varepsilon = \left(S'_{22} + S'_{12}\frac{S'_{22} - S'_{12}}{S'_{11} - S'_{12}}\right)\sigma'_{22} = \frac{1}{M_2}\sigma'_{22} \tag{11}$$

Here $M_i$ is equivalent to $E$ in the uniaxial stress state and referred to as the biaxial modulus.

For a planar isotropic material, $\sigma'_{11} = \sigma'_{22} = \sigma$ and hence $S'_{11} = S'_{22}$ the biaxial moduli becomes

$$M_1 = M_2 = 1/(S'_{11} + S'_{12}) = \frac{E}{1 - \upsilon} \tag{12}$$

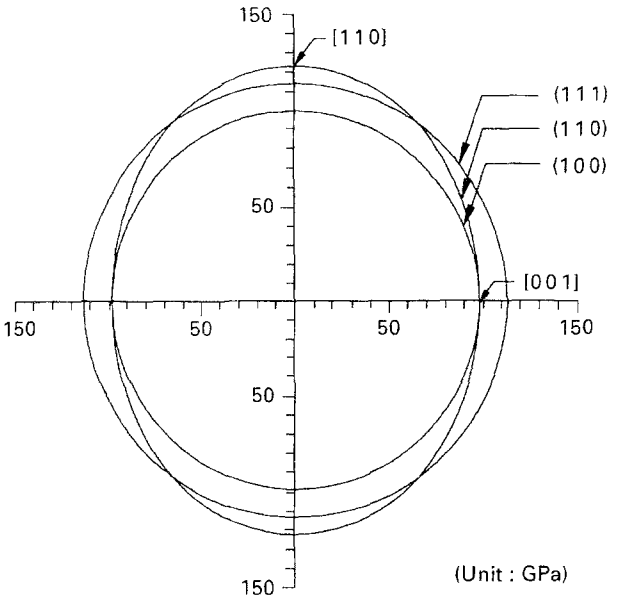


*Figure 8* Calculated biaxial elastic moduli of (100), (110) and (111) planes of aluminium.

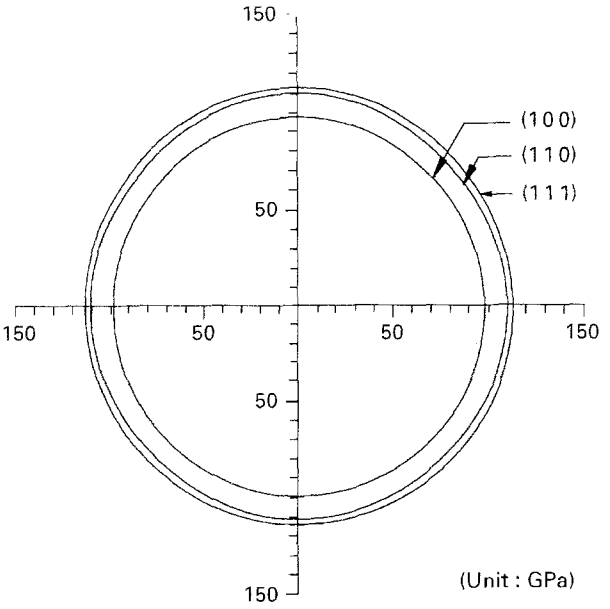


*Figure 9* Calculated average biaxial elastic moduli of (100), (110) and (111) planes of aluminium.

because $1/S'_{11} = E$ and Poisson's ratio $v$ is equal to $-S'_{12}/S'_{11}$. In this case Equations (10) and (11) reduce to

$$\sigma = \frac{E}{1 - v}\varepsilon \tag{13}$$

This equation clearly shows that the biaxial modulus is equivalent to Young's modulus $E$ in the uniaxial stress.

However, for anisotropic materials, $M_1$ and $M_2$ are not always independent of orientation. Fig. 8 shows the biaxial moduli calculated along the (100), (110) and (111) planes of aluminium. The biaxial moduli along the (100) and (111) planes are independent of direction, whereas the modulus along the (110) plane varies with orientation. It will be convenient to define a modulus which is independent of direction.

The strain energy of a cubic material under the equibiaxial strain-plane stress condition can be expressed as

$$W = \tfrac{1}{2}(\sigma'_{11} + \sigma'_{22})\varepsilon \tag{14}$$

It follows from (10) and (11) that

$$W = \tfrac{1}{2}(M_1 + M_2)\varepsilon^2 \tag{15}$$

Since energy is a non-directional quantity, the quantity of $(M_1 + M_2)$ must be non-directional. Fig. 9 shows the calculated value of $(M_1 + M_2)/2$, that is, the average value of $M_1$ and $M_2$, along the (100), (110) and (111) planes. It is noted that the average biaxial modulus along the (110) plane is non-directional. The biaxial elastic moduli in Fig. 6 are the average moduli. It can be seen from Fig. 6 that the minimum biaxial moduli is obtained along the (100) plane.

## References


1. T. MATSUZAKI and T. YAMAZAKI, *Fujitsu Scientific and Technical Journal* **6** (1980) 45.
2. K. HIRATA and T. YAMASAKI, IEEE *Trans on Parts, Hybrids and Packaging*, PHP **12** (1976) 217.
3. R. S. ALWITT, H. UCHI, T. R. BECK and R. C. ALKIRE, *J. Electrochem. Soc.* **138** (1984) 13.
4. C. G. DUNN and R. B. BOLON, *ibid.* **116** (1969) 1050.
5. K. R. HEBERT and R. C. ALKIRE, *ibid.* **135** (1988) 2447.
6. C. K. DYER and R. S. ALWITT, *ibid.* **128** (1981) 300.
7. B. J. WIERSMA, Y. TAK and K. R. HEBERT, *ibid.* **138** (1991) 371.
8. N. F. JACKSON, *Electrocomponent Science and Technology*, **2** (1975) 33.
9. R. S. ALWITT, *J. Electrochem. Soc.* **118** (1971) 1730.
10. R. K. HART, *Trans Faraday Soc.* **53** (1957) 1020.
11. W. VEDDER and D. A. VERMILEA, *ibid.* **65** (1969) 567.
12. H. TAKAHASHI, Y. UMEHARA, T. MIYAMAMOTO, *J. Surf. Fin., Jpn* **38** (1987) 67.
13. R. K. HART, *Proc. Roy. Soc. London, Ser. A* **236** (1956) 68.



*Received 16 May 1994*
*and accepted 9 November 1995*